# PCCP

## Accepted Manuscript

This is an *Accepted Manuscript*, which has been through the Royal Society of Chemistry peer review process and has been accepted for publication.

*Accepted Manuscripts* are published online shortly after acceptance, before technical editing, formatting and proof reading. Using this free service, authors can make their results available to the community, in citable form, before we publish the edited article. We will replace this *Accepted Manuscript* with the edited and formatted *Advance Article* as soon as it is available.

You can find more information about *Accepted Manuscripts* in the Information for Authors.

ROYAL SOCIETY OF CHEMISTRY

www.rsc.org/pccp

# Physical Chemistry Chemical Physics

## ARTICLE

# Effect of Negative Pressure Aging on Aggregation of Cu2O Nanoparticle and Its Application to the Laser Induced Copper Electrode Fabrication

H. S. Lee and M. Y. Yang*

Aggregation and dispersion of nanoparticle are critical problems in selective laser sintering. In this study, negative pressure aging was applied to resolve an aggregation of nanoparticle and metal oxide reduction method was used to make a well-dispersed nanoparticle in solvent. As a result, metal oxide nanoparticle was synthesized according to a grade of the aggregation and an aging condition was found out that which is well-dispersed condition of nanoparticle in solvent with less redissolution of nanoparticle. Furthermore, a coating quality and characteristics of laser induced sintering were analyzed according to the grade of the aggregation. The coating quality was affected by the aggregation and a statistical dispersion of nanoparticle. The coating deposited by particles with wide statistical dispersion has better quality comparing with the coating from particle with narrow dispersion. The quality of laser sintered electrode depends on the aggregation but the dependency of the aggregation diminished as an irradiation of the laser power goes down.

## Introduction

Recently, electrode requires high conductivity and narrow pattern width to satisfy a trend of high density integration of electronic devices. Photolithography and vacuum deposition are representative process of the electrode fabrication and they have outstanding quality and reproducibility. These processes, however, have drawbacks such as high processing cost and use of toxic reagent. For these reasons, printed electronics using a nanoparticle comes to the forefront as an alternative process such as roll to roll printing[1,2], inkjet printing[3-5], selective laser sintering[6,7] and so on. Among them, selective laser sintering receives attention in terms of easy process without mask, low damage on substrate, and concise setup of process. In the selective laser sintering, conductivity of electrode pattern and reproducibility of the process are significant evaluation index of the process, and aggregation of nanoparticle affects dominantly to the evaluation index. In previous studies of nanoparticle synthesis, reaction time[8,9] and reagent concentration[10] are optimized to prevent the aggregation of nanoparticle, or mechanical breakage methods[11-14] are applied to break the aggregation of nanoparticle in post-process of the synthesis. These of methods, however, need toxic reagent or additional process, respectively. On the other hand, Ostwald ripening[15,16] breaks the aggregation of nanoparticle during in synthesis and do not need any other additional reagent or process, but it depletes yield of nanoparticle too. Hence, in this study, negative pressure aging was adopted to delay the depletion of nanoparticle during the Ostwald ripening in synthesis, and then

the synthesized nanoparticle was analyzed to confirm an influence of the aging. After that, the selective laser sintering process was done to verify the effect of aggregation in the process.

## Experiment

### Preparation of coppe(I) oxide nanoparticle

All reagent and method refer to common copper(I) oxide synthesis in publications[8-10,15,16] and all of the reagent purchased from Aldrich. 74mM of CuCl2, 75mM of D-glucose, and 1.25mM of PVP are dissolved sufficiently in an aqueous solution of a 500ml round flask and heated at 100℃ for an hour with vigorous stirring. After that, 187mM of NaOH aqueous solution was poured into the round flask using a syringe with or without plugging a rubber stopper to make a pressure difference in the aging process. The solution of aggregated copper(I) oxide with small particle sizes quickly moves into cool water of about 4 ℃ to prevent additional growth of nanoparticles and stirred vigorously to make a turbulent flow for breakage of aggregation during different hours as shown in S1. When plugging a rubber stopper into the flask, the temperature dropping of the closed flask spontaneously creates negative pressure inside the flask, because the swelled solvent inside the flask shrinks as the temperature drops to that of ambient air.

After the nanoparticle has sufficiently aged, the nanoparticle centrifuged at 8000 rpm for 20 minutes and was washed three times with water and ethanol. After that, the nanoparticle was dispersed in butanol to prevent an oxidation of the nanoparticle. The dispersed nanoparticle was coated on glass at 2500rpm for 40 seconds using a spin coating method to ensure coating

Department of Mechanical Engineering, Korea Advanced Institute of Science and Technology, Daejeon, 305-701, Republic of Korea
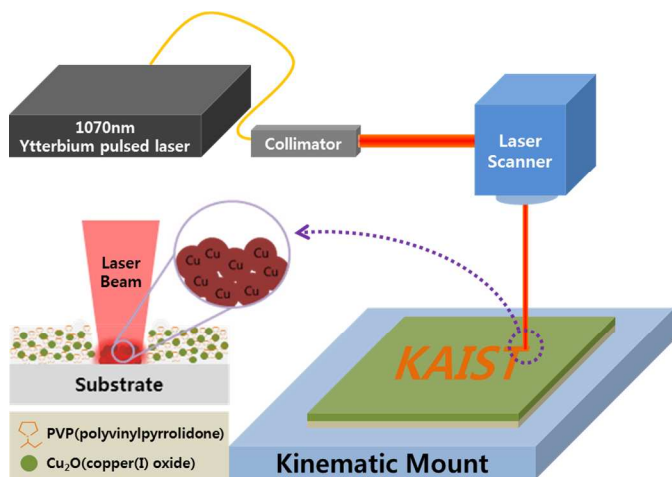
**Fig. 1** Schematic of concise copper electrode fabrication system and mechanism of laser induced nanoparticle sintering.

uniformity and effect of aggregation. After the measurement of morphology and particle size distribution, the copper(I) oxide dried in a vacuum chamber for two days to measure the purity and the yield of the copper(I) oxide nanoparticle in each condition.

**Copper electrode fabrication**

1g of copper(I) oxide nanoparticle and 1g of PVP powder are dispersed in 10ml of alcohol solvent and the mixture is shaken by a mixer for a day. The solution of copper(I) oxide nanoparticle is coated on glass using a spin coater at 2500 rpm for 50 seconds. The glass with copper(I) oxide coated solution is heated by a 1070 nm pulsed laser to reduce the copper(I) oxide to copper as shown in Fig. 1 and the reaction is as shown below[17].

$$Cu_2O + HCOOH \rightarrow 2Cu + H_2O + CO_2 \qquad (1)$$
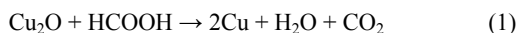
After the laser irradiation, the glass is rinsed by DI water and is dried by high pressure air in normal atmosphere.

**Characterization**

After washing process of each experiment, TEM(FEI, Tecnai G2 F30 S-Twin), SEM(FEI, Nova230), and Particle size analyzer(Otsukael, ELS-Z2) were used to determine a state of agglomeration and morphology of the copper(I) oxide particle. Purity of the copper(I) oxide nanoparticle was measured using an X-ray diffraction (Rigaku, D/MAX-RB) and a yield of each synthesis was measured using an electronic scale(Vibra, AJH-620E-D). To observe a morphological difference of the mixtures at each step of the synthesis and conditions, the absorbance of solutions was measured using a UV-VIS spectrometer(Thermo Scientific, Evo-220 PC control). Finally, the copper(I) oxide nanoparticles coated on glass were measured using a confocal optical profiler(Nanofocus, μsurf) to verify coating uniformity, morphology, and roughness of coated surface.

## Result and discussion

**Breakage of aggregated copper(I) oxide nanoparticle using a negative pressure aging**

Copper(I) oxide is well known promising material not only for p-type semiconductor[18], photovoltaic material[19], and anti-bacterial material[20], but also for precursor of copper electrode[17]. For these kinds of purpose, there are so many synthesis methods[21-25] to make a well-shaped copper(I) oxide nanoparticle, but they are mostly focused on how to make a well-shaped nanoparticle using a good surfactant and solvent or a facet controlled nanoparticle with proper surfactant in a low copper ion concentration even though the aggregation of nanoparticle still existed in synthesis.

Copper(I) oxide nanoparticle solution shows a dark green color just after finalization of the reaction of nucleation with reduction agent at high temperatures, and the color gradually turns to orange and finally it becomes reddish brown at the beginning of the aging of the solution. The change of the color reflects the agglomeration of the copper(I) oxide[21,26]. Schematics of the aging in copper(I) oxide nanoparticle synthesis are shown in Fig. 2, according to aging period and aging pressure. At the aging process, chemical potential of the reaction chamber changes rapidly and it causes drastic Ostwald ripening. The difference of chemical potential before and after the reaction is described by[27]

$$\mu = \mu_0 + \alpha \cdot \Delta T + \beta \cdot \Delta P \qquad (2)$$

where μ is chemical potential, $\mu_0$ is initial chemical potential, α is temperature coefficient, ΔT is temperature change after reaction, β is pressure coefficient, ΔP is pressure change after reaction. The Ostwald ripening means that not only nanoparticles are redissolved in solvent but also aggregated nanoparticles are separated each other in this process[15,16]. In normal pressure aging condition, without plugging a rubber stopper, the chemical potential increased rapidly because α·ΔT drops to ambient condition according to the reaction chamber cools down. In negative pressure condition, however, the chemical potential increased slowly because the β·ΔP drops down with a rising of α·ΔT as shown in Fig. S2 and Table 1. Differences of the color change between negative pressure aging and normal pressure aging means that the normal pressure aging has redissolved copper ion in its solution during the aging period caused by Ostwald ripening, and the redissolved nanoparticle increases until the nanoparticle is fully dissolved in solvent or the nanoparticle becomes a lump of copper(I) oxide. On the other hand, the negative pressure aging
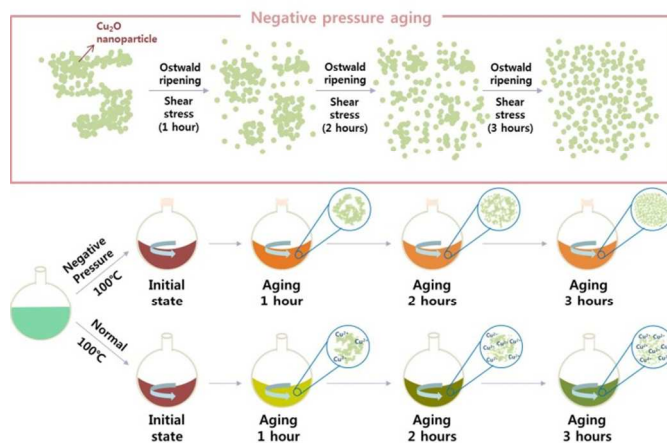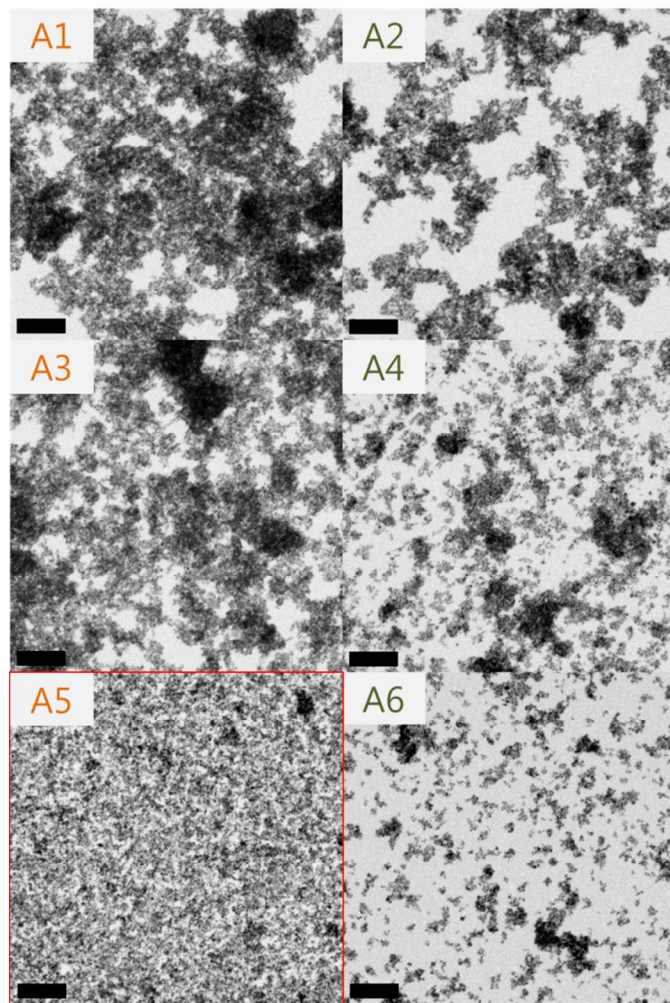


**Fig. 2** Schematics of the difference between negative pressure aging and normal pressure aging in copper(I) oxide nanoparticle synthesis.

**Table 1** Measurement of the temperature and the pressure of the chamber during the negative pressure aging process.

|  | Aging 0h | Aging 1h | Aging 2h | Aging 3h |
|---|---|---|---|---|
| Temperature (℃) | 100 | 26.2 | 24.5 | 23.6 |
| Pressure (-Mpa) | 0 | 0.084 | 0.083 | 0.082 |



**Fig. 3** TEM images of the negative pressure and normal pressure aging according to the aging duration (▬: 1μm).

reveals a color change only from the beginning of the aging(reddish brown) to one hour after aging(orange) because the negative pressure attenuates the change of chemical potential and the attenuated chemical potential delays Ostwald ripening. This phenomenon is ascertained during measurements.

At first, the aggregation of the copper(I) oxide nanoparticle is verified roughly by TEM images as shown in Fig. 3 and HRTEM images in Fig. S3. In the state of after having aged by one hour, the copper(I) oxide nanoparticle shows serious aggregation in both negative pressure condition and normal pressure condition. The aggregation becomes more reduced as aging continues in both negative pressure and normal pressure aging but the normal pressure aging shows less nanoparticles gradually in the scanning area than the negative pressure aging, because faster denucleation occurred by a ripening phenomenon under normal conditions. It means that the

negative pressure results in a delay of the redissolution of nanoparticles.

The denucleation (or redissolving) of the nanoparticle is quantitatively proven by a measurement of the yield of the nanoparticle as shown in Fig. 4(a). Regarding negative pressure aging, the yield of the nanoparticle has barely decreased as aging continues, but the normal pressure aging shows a dramatic reduction of the nanoparticle according to aging period. It means that the negative pressure attenuates the chemical potential variations as the temperature of the flask drops close to the temperature of ambient air. On the other hand, normal pressure aging has experienced significant denucleation as the temperature of the flask drops closer to ambient temperature until around 2 hours of aging and then the denucleation becomes slower. Consequently, just 50 percent of the nanoparticle remains after 3 hours of aging during normal pressure synthesis.

A breakage of the aggregation and the ripening are figured out in more detail using a particle size analysis as shown in Fig. 4(b). The mean size gradually decreased according to the aging time but the standard deviation increased according to the aging time. In addition, exceptionally, the negative pressure aging 1 hour shows highest standard deviation because the standard deviation is affected by not only deviation between group of samples but also the number of the groups. The negative pressure aging 1 hour has lowest number of groups and it makes the standard deviation larger than others. The aggregated
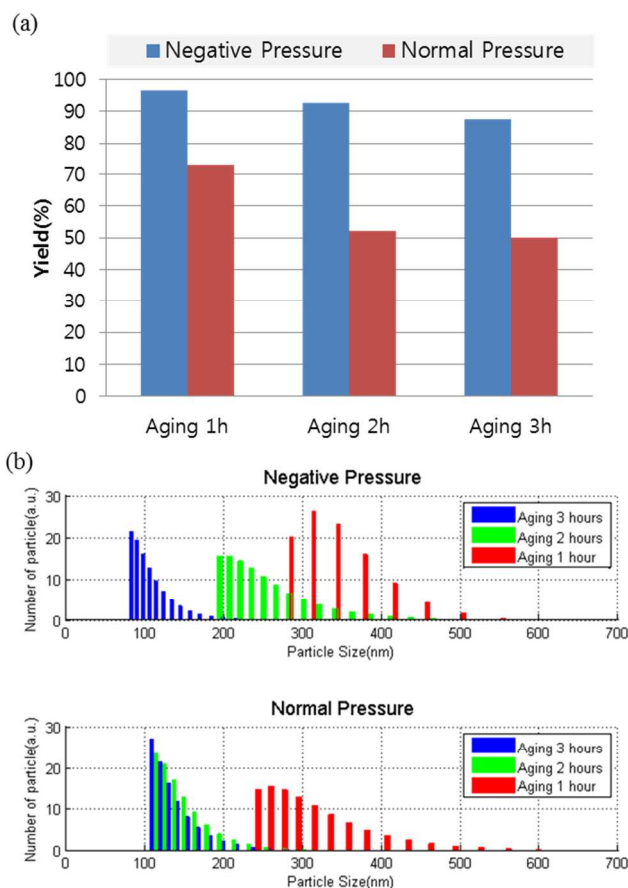


**Fig. 4** Qualitative analysis of the copper(I) oxide synthesis according to the grade of aggregation. (a) Yields of copper(I) oxide nanoparticles and (b) Particle size distribution of the copper(I) oxide nanoparticle dispersed in butanol.

nanoparticle after aging for one hour of negative pressure aging shows rough and wide distribution from a size of 280 nm to 550nm(Mean Diameter: 345nm, Standard Deviation: 10). After an hour, however, the nanoparticles has a distribution from a size of 190 nm to 450 nm(M.D.: 249nm, S.D.: 5.5) caused by a breakage of aggregated nanoparticles to a smaller aggregated nanoparticle with less change of size distribution range. The copper(I) oxide nanoparticle finally exists a range from a size of 80 nm to 220nm(M.D.: 106nm, S.D.: 7) after 3 hours of aging in negative pressure aging and that has a narrower particle size range than before the state of having aged 2 hours. Also, the peak of size distribution is getting sharper at the size of 80 nm than the size of 220 nm. This trend of particle size distribution means that the breakage of aggregation works throughout the entire aging process and the aging causes a decrease of size of aggregated nanoparticle after having aged an hour, to a size of 280 nm to 550 nm, and after having aged by 3 hours, to a size of 80 nm to 220 nm. Regarding normal pressure aging, however, the particle size distribution represents a different size distribution. At the state of having aged by one hour, it shows a broad size distribution from a size of 250 nm to 600 nm(M.D.: 313nm, S.D.: 5.6), and then the nanoparticle quickly breaks after an hour, from a size of 115 nm to 510 nm(M.D.: 145nm, S.D.: 7.7). The final state of normal pressure aging, however, shows a little change of the particle size distribution from a size of 109nm to 512nm(M.D.: 136nm, S.D.: 8) because the chamber was saturated by the excessive redissolving of nanoparticle. Consequently, the breakage of the aggregated nanoparticle by the Ostwald ripening depends on its chemical potential and concentration of the synthesis solution.

The breakage of the copper(I) oxide nanoparticle can also be confirmed by measuring the absorbance of the nanoparticle. There are 3 peaks(around a wavelength of 290 nm, 370 nm, and 450 nm) in general when copper(I) oxide has a particle size of up to 50 nm or has special structures[28-30]; the peaks caused by higher-order modes at Mie scattering resonance[22]. As shown in Fig. 5(a), the intensity of the peaks changes according to the grade of aggregation and concentration of the nanoparticles.

In both negative pressure aged and normal pressure aged nanoparticles, the peak around a wavelength of 450 nm diminishes according to both the breakage of the aggregation and decrease of the number of nanoparticles. On the other hand, the peaks around a wavelength of 290 nm and 370 nm are elevated according to the nanoparticles take part from each other. The excessive denucleation of the conditions of A4 and A6 show a less difference of intensity than the negative pressure conditions but the intensity difference among the 3 peaks still exists and the deviation of the peaks are bigger after having aged 3 hours and 2 hours, than from having aged one hour, because of the breakage of aggregation.

Under normal pressure aging, the excessive denucleation reveals that the copper(I) oxide nanoparticle is redissolved and creates another composite which causes a diminution of the yield during the process. The composite is compared with a composite of negative pressure aging and copper(I) nanoparticle as shown in Fig. 5(b). At first, copper(I) oxide nanoparticle has a peak of around wavelength of 450 nm, as mentioned in fig. 5(a) and the bluish remaining composite of the normal pressure condition has a broad peak of around wavelength of 520 nm to 820 nm as shown in Fig. 5(d) which is a copper complex ion peak, such as $(Cu(OH)_4)^{2-}$ ion[26] and diclofenac[31]. Also, in Fig. 4(c), the yellowish remaining composite of the negative pressure aging is ascertained to have a sodium chloride solution peak of around wavelength of 550
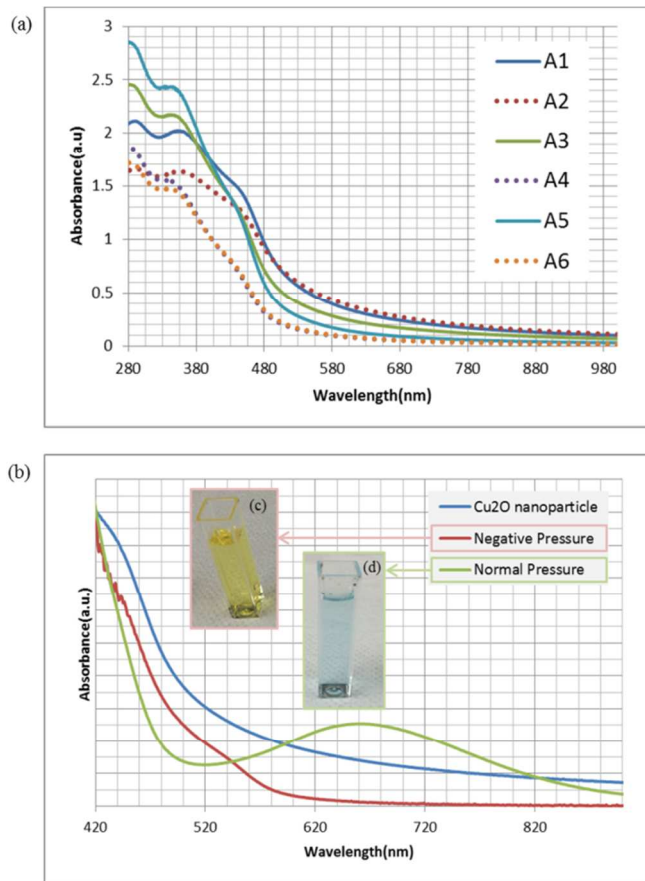


**Fig. 5** (a) Absorbance of the copper(I) oxide nanoparticle according to aging period and aging pressure using a method of direct transmittance measurement without absorbance of solvent. (b) Absorbance of the copper(I) oxide nanoparticle, remaining composite of solution of negative pressure condition, and remaining composite of solution of normal pressure condition except for absorbance of solvent.

nm[32]. The yellowish color is due to uncentrifuged copper(I) oxide nanoparticles which are trapped by the high surface tension of water and it also causes a little of reduction of the yield in negative pressure aging.

The change of yield, include the excessive denucleation, can also be affected by a constructing of another composited nanoparticle such as copper(II) oxide or copper hydroxide in copper(I) oxide nanoparticle. To ensure the purity of the synthesis, crystal structures of an each condition of the nanoparticle are measured as shown in Fig. S4. As a result, all of the synthesized nanoparticles have pure cuprite crystal structures and also the full-width at half maximum of the XRD patterns are almost the same. According to the scherrer equation, it means that not only each of the nanoparticles in different conditions have similar particle sizes and crystal structures[28] but also the ripening functions more as an aggregation breaker of nanoparticle[15] than a role of particle growing[34].

### Relation of coating quality and aggregation of nanoparticle

Aggregation generally affects coating uniformity and the roughness of a solution processed thin film. Therefore, the quality of the coated nanoparticle can be evidence of aggregation and vice versa. As mentioned in previous chapter,
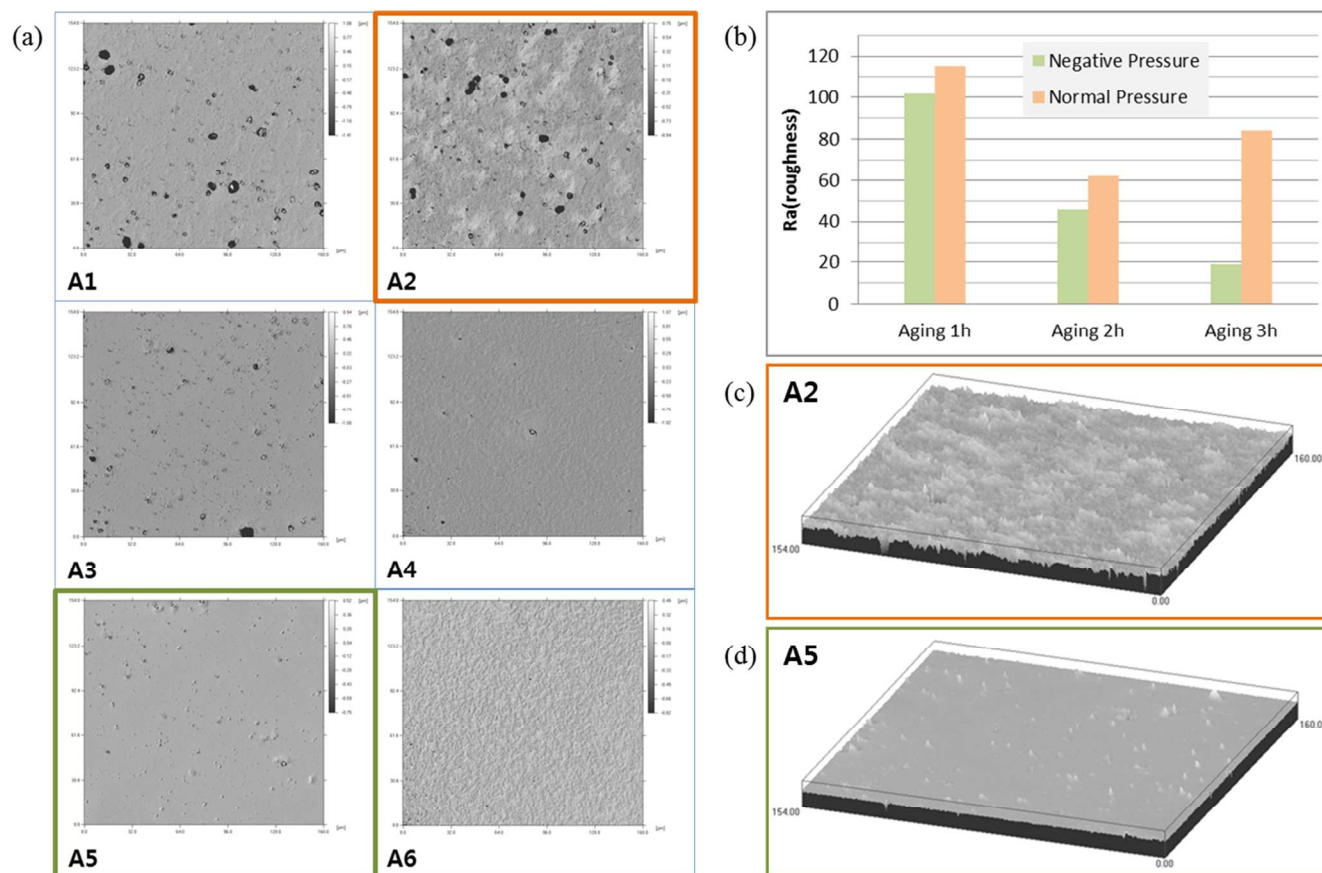
**Fig. 6** Measurement of the coating quality of the copper(I) oxide nanoparticle. (a) Images of the coated copper(I) oxide nanoparticle on glass using a spin coating method (size of the measurement: 154μm(h)*160μm(w)). (b) Roughness of the coated copper(I) oxide nanoparticles. (c) Comparison of the best and worst roughness of the coated copper(I) oxide nanoparticles.

the aggregation of nanoparticle was clearly classified by the mean diameter and the standard deviation according to the aging time in both negative pressure synthesis and normal pressure synthesis. Each of the synthesis was coated on glass to evaluate the aggregation of nanoparticle and to predict an effect of the aggregation to the laser induced electrode fabrication in practice. As shown in Fig. 6(a), coating quality has a similar trend of the result of the TEM images. Aggregated particles exist on the surfaces and the aggregation improves as the aging time of sample is longer. Furthermore, conditions of A4 and A6 have bumpy morphology on the surface because of thinner thickness of the coated nanoparticle than others which caused by a low concentration of the conditions. Roughness of the coated nanoparticles is also compared as shown in Fig. 6(b). The particle size distributions are uniformly distributed according to the aging time in negative pressure. At first, the roughness is gradually reduced from A1, 102 nm, to A5, 19 nm, in negative pressure aged nanoparticles. It means that the roughness is proportionate to the grade of aggregation. Regarding normal pressure aged nanoparticles, the roughness was improved until the 2 hours aged nanoparticle, but it became worse again in the 3 hours aged nanoparticle even though the mean diameter of the nanoparticle was decreased because the standard deviation is higher than the 2 hours aged nanoparticle. In consequence, normal pressure aging condition has a relatively worse roughness than negative pressure aging even when the normal pressure aging condition has a less aggregated particle than
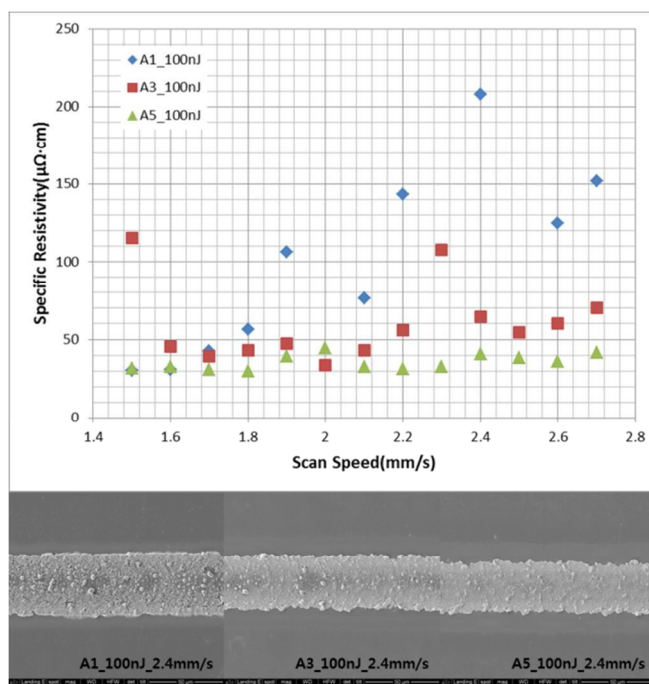


**Fig. 7** Comparison of electrical resistivity and shape of the fabricated copper electrode pattern according to the grade of aggregation of nanoparticle.
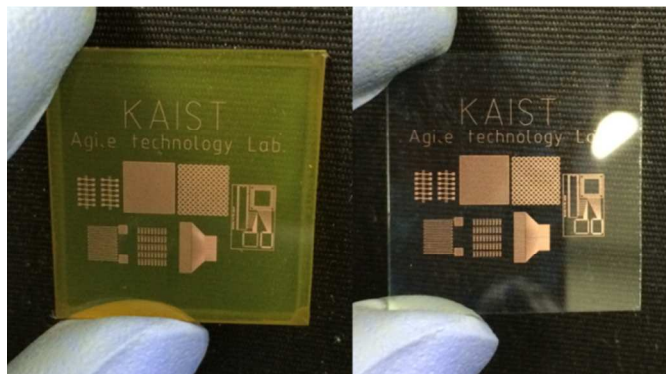
**Fig. 8** Copper electrode on glass substrate(1 inch × 1 inch) made by a reduction of copper(I) oxide nanoparticles which has water washable characteristics.

negative pressure. It means that the highly concentrated nanoparticle ink has better roughness because the high concentration of nanoparticles accumulates more nanoparticles in direction to the thickness than low concentration of nanoparticle and flattening is occurred in roughness. Hence, it is confirmed that the roughness is affected by the aggregation of nanoparticle, the particle size distribution, and the thickness of the coated particle.

### Laser sintering according to the grade of aggregation of nanoparticle

As shown in previous chapter, the copper(I) oxide nanoparticle shows a different grade of aggregation according to aging time and it transfers to the coating quality of copper(I) oxide nanoparticle. Consequently, a relationship between aggregation of nanoparticles and fabrication of laser induced metal electrode were figured out to confirm that the aggregation effects to characteristics of electrode pattern. The copper(I) oxide nanoparticle A1, A3, and A5 were prepared to compare the patterns according to the grade of aggregation and photon energy of NIR laser was irradiated to the compounds of the copper(I) oxide nanoparticle and PVP. As shown in Fig. 7, A5, least aggregated nanoparticle, has a best pattern shape and electrical conductivity which is not depends on a fluence of laser energy. Furthermore, a width of the pattern is getting narrower when the aggregation of nanoparticle is fewer. The width is affected by a breakage of aggregation which affect to an increasing of viscosity and the viscosity is inverse proportional to Marangoni number. On the other hands, a conductivity of most aggregated nanoparticle, A1, has a drastic change as the fluence of laser energy. The condition of A1 also shows an irregular and a discontinuous conductivity according to the fluence because there are too many aggregated nanoparticles in solvent and it also causes an unstable reproducibility of copper electrode fabrication.

Therefore, a condition of A5 was adopted for making an electrode pattern to evaluate its possibility as an electrode. As shown in Fig 8, the copper(I) oxide nanoparticle compound coated uniformly on glass and laser irradiated areas were reduced and sintered effectively to copper electrode. Furthermore, remains of the copper(I) oxide around laser irradiated area was washed easily by deionized water. It means that the total fabrication process of copper electrode using the copper(I) oxide is eco-friendly too.

### Conclusion

Aggregation of nanoparticle, dispersion of nanoparticle solution, and reproducibility of process remain as a problem awaiting solution in printed electronics. In this study, copper(I) oxide nanoparticle for laser sintering process was synthesized with a negative pressure aging to control not only the aggregation of nanoparticle but redissolution of it. After that, the aggregated nanoparticles were coated on a substrate and fabricated a copper electrode using a laser to compare a difference of electrode quality according to the aggregation of nanoparticle. As a result, copper(I) oxide nanoparticle with negative pressure aging shows high yield, and less aggregation than normal pressure aging. Spectroscopic characteristic was changed according to the aggregation and the concentration of nanoparticle. Roughness of the coated nanoparticle shows a better quality when the aggregation is little, the statistical dispersion is broad, and the thickness is thick. Electrical conductivity is higher when the aggregation is lower but the difference of the conductivity diminishes according to the decrease of the laser fluence.

### Notes and references

1  M. Hösel and F. C. Krebs, *J. Mater. Chem.*, 2012, **22**, 15683.
2  D. Angmo, T. T. Larsen-Olsen, M. Jørhensen, R. R. Søndergaard and F. C. Krebs, *Adv. Energy Mater.*, 2013, **3**, 172.
3  J. Perelaer, R. Abbel, S. Wünscher, R. Jani, T. V. Lammeren and U. S. Schubert, *Adv. Mater.*, 2012, **24**, 2620.
4  J. T. Wu, S. L. C. Hsu, M. H. Tsai and W. S. Hwang, *J. Phys. Chem. C*, 2011, **115**, 10940.
5  S. Jeong, H. C. Song, W. W. Lee, S. S. Lee, Y. Choi, W. Son, E. D. Kim, C. H. Paik, S. H. Oh and B. W. Ryu, *Langmuir*, 2011, **27**, 3144.
6  S. H. Ko, H. Pan and C. P. Grigoropoulos, *Appl. Phys. Lett.*, 2007, **90**, 141103.
7  M. Aminuzzaman, A. Watanabe and T. Miyashita, *J. Nanopart. Res.*, 2010, **12**, 931.
8  B. K. Park, S. H. Jeong, D. J. Kim, J. H. Moon, S. W. Lim and J. S. Kim, *J. Col. Int. Sci.*, 2007, **311**, 417.
9  C. H. Kuo and M. H. Huang, *Nano today*, 2010, **5**, 106.
10  C. H. Kuo and M. H. Huang, *J. Phys. Chem. C*, 2008, **112**, 18355.
11  S. I. Ana, P. S. Isabel, P. J. Jorge, R. G. Benito, G. A. F. Javier and L. M. Luis M., *Adv. Mater.*, 2006, **18**, 2529.
12  L. Katharina, *Adv. Mater.*, 2001, **13**, 765.
13  R. Murakami, H. Moriyama, M. Yamamoto, B. P. Binks and A. Rocher, *Adv. Mater.*, 2012, **24**, 767.
14  S. H. Jeong, S. H. Lee, Y. J. Jo, S. S. Lee, Y. H. Seo, B. W. Ahn, G. M. Kim, G. E. Jang, J. U. Park, B. H. Ryu and Y. M. Choi, *J. Mater. Chem. C.*, 2013, **1**, 2704.
15  L. Zhang and H. Wang, *ACS nano*, 2011, **5**, 3257.
16  L. Zhang and H. Wang, *J. Phys. Chem. C.*, 2011, **115**, 18479.
17  J. E. Ryu, H. S. Kim and H. Thomas Hahn, *J. Elec. Mater.*, 2011, **40**, 42.

18  N. Michael and E. Simon D, *Phy. Chem. Chem. Phys.*, 2006, **8**, 5350.

19  H. M. Wei, H. B. Gong, L. Chen, M. Zi and B. Q. Cao, *J. Phys. Chem. C*, 2012, **116**, 10510.

20  Y. J. Lee, S. Kim, S. H. Park, H. Park and Y. D. Huh, *Mater. Lett.*, 2011, **65**, 818.

21  L. I. Hung, C. K. Tsung, W. Huang and P. Yang, *Adv. Mater.*, 2010, **22**, 1910.

22  X. Meng, G. Tian, Y. Chen, Y. Qu, J. Zhou, K. Pan, W. Zhou, G. Zhang and H. Fu, *RSC Adv.*, 2012, **2**, 2875 .

23  Y. Xu, H. Wang, Y. Yu, L. Tian, W. Zhao and B. Zhang, *J. Phys. Chem. C*, 2011,  **115**, 15288.

24  Q. Hua, K. Chen, S. Chang, Y. Ma and W. Huang, *J. Phys. Chem. C*, 2011, **115**, 20618.

25  W. C. Huang, L. M. Lyu, Y. C. Yang and M. H. Huang, *J. Am. Chem. Soc.*, 2012, **134**, 1261.

26  Z. Zhang, H. Che, Y. Wang, J. Gao, L. Zhao, X. She, J. Sun, P. Gunawan, Z. Zhong and F. Su, *Ind. Eng. Chem. Res.*, 2012, **51**, 1264.

27  G. Job and F. Herrmann, *Eur. J. Phys.*, 2006, **27**, 353

28  C. Y. Christopher and C. Z. Hua, *Chem. Mater.*, 2012, **24**, 1917.

29  P. He, X. Shen and H. Gao, *J. Col. Int. Sci.*, 2005, **284**, 510.

30  J. Gao, Q. Li, H. Zhao, L. Li, C. Liu, Q. Gong and L. Qi, *Chem. Mater.*, 2008, **20**, 6263.

31  R. L. Souze and M. Tubino, *J. Braz. Chem. Soc.*, 2005, **16**, 1068.

32  T. Suzuki, Y. Hirahara, K. Bunya and H. Shinozaki, *J. Mater. Chem.*, 2010, **20**, 2773.

33  P. Krawiec, P. L. Cola, R. Gläser, J. Weitkamp, C. Weidenthaler and S. Kaskel, *Adv. Mater.*, 2006, **18**, 505.

34  H. Xu, W. Wang and L. Zhou, *Cryst. Growth Des.*, 2008, **8**, 3486.

**Physical Chemistry Chemical Physics Accepted Manuscript**